Medium-energy ion-scattering study of a possible relation between the Schottky-barrier height and the defect density at $NiSi_2$/Si(111) interfaces

J. Vrijmoeth and J. F. van der Veen
FOM Institute for Atomic and Molecular Physics, Foundation for Fundamental Research on Matter, Kruislaan 407, 1098 SJ Amsterdam, The Netherlands

D. R. Heslinga and T. M. Klapwijk
Department of Applied Physics, University of Groningen, Nijenborgh 18, 9747 AG Groningen, The Netherlands
(Received 30 April 1990)

We have studied the electrical properties of both orientations of the $NiSi_2$/Si(111) interface in relation to the atomic structure at the very interface. The flat-band Schottky-barrier heights corresponding to the *A*- and *B*-type oriented silicides are shown to be 0.65 and 0.81 eV, respectively, in agreement with the literature. Measurements using medium-energy ion scattering show that the concentrations of atoms displaced from lattice sites at the *A*- and *B*-type oriented $NiSi_2$/Si(111) interfaces are smaller than $\sim 1\times 10^{13}$ Si atoms cm^{-2} and $\sim 3\times 10^{13}$ Si atoms cm^{-2}, respectively, ruling out the possibility that the difference in Schottky-barrier height is caused by defects. The difference should therefore be intrinsically related to the interfacial atomic geometry.

I. INTRODUCTION

Since the discovery of the rectifying property of a point-contact device, much work has been devoted to the unraveling of the formation mechanism of the energy barrier for electron transport across a metal-semiconductor interface, the so-called Schottky barrier.[1-6] The electronic behavior of a metal-semiconductor system is not only influenced by the bulk properties (e.g., work function and electronegativity) of metal and semiconductor, but also by the structural properties of the metal-semiconductor interface (e.g., defects, giving rise to interface states which pin the Fermi level in the band gap).

The development of theory for Schottky-barrier formation has been guided by the observed chemical trends in barrier heights of different metal-semiconductor combinations. The original Schottky-Mott proposal that the barrier height equals the difference between the metal work function and the semiconductor electron affinity does not hold,[1,2] but this parameter *does* correlate with the barrier height for many metal-semiconductor combinations.[6] Bardeen[3] recognized that electronic states in the band gap had to be invoked to account for the relatively weak dependence of the Schottky-barrier height on this difference. Over the years many theories attempting to identify the nature of these interface states have been proposed.[4-9] However, so far none of the theories proposed seems to provide an indisputable and complete explanation of the experimental data. This is largely because interface states arise from a variety of subtle structural features, such as impurities and defects. Experimentally, it is difficult to characterize these properties to the required level of detail. This makes it difficult to compare the electrical properties of different metal-semiconductor combinations. Clearly, the understanding of the fundamental parameters governing Schottky-barrier formation would greatly benefit from experiments on "model" metal-semiconductor contacts which form a uniform atomically well-ordered interface over the entire semiconductor surface area; for such a model system, all structural properties would be known.

Recently, model systems have become available due to the possibility of growing epitaxially the disilicides of Ni and Co on Si(111) under UHV conditions with a high degree of crystalline perfection. Epitaxial $NiSi_2$ offers an additional feature: It has been shown to grow in two orientations with respect to a Si(111) substrate, namely the so-called type-*A* orientation, in which the silicide has the same orientation as the substrate, and the type-*B* orientation, in which the silicide is rotated over 180° with respect to the substrate around the surface normal.[10] The silicide orientation can be influenced by an appropriate choice of the initial amount of Ni evaporated. The $NiSi_2$/Si(111) interfaces are well characterized on an atomic scale: For both silicide interface orientations there appears to be agreement on structure models in which the interface Ni atoms are seven-fold coordinated.[11-15] The only difference between the two systems is the atomic arrangement at the interface; the bulk properties of the constituting materials are of course identical.

Measurements of the Schottky-barrier heights of these well-defined interfaces, however, have resulted in a controversy. Tung *et al.*[16,17] reported the barrier heights for *A*-type $NiSi_2$/Si(111) (0.65 eV on *n*-type doped Si) to differ by 0.14 eV from that of *B*-type (0.79 eV on *n*-type

Si); these authors attributed this difference in electronic behavior to the difference in atomic arrangement at the interface. This conclusion, however, was challenged by Liehr *et al.*,[18] who asserted that the Schottky-barrier heights are related to the structural perfection of the silicide-silicon interfaces prepared. These authors observed barrier heights of 0.78 eV, not only for *A*- and *B*-type oriented interfaces, but occasionally even for a so-called "*C*-type" NiSi/Si(111) interface. Less-perfect, e.g., mixed *A*- and *B*-type interfaces resulted in lower barrier heights ($\sim$0.66 eV). An observed lower barrier height for *A*-type oriented $NiSi_2$/Si(111) interfaces would, according to this work, be caused by a higher density of interface defects; a higher defect density at the *A*-type interface as compared to the *B*-type one is consistent with the fact that the former is higher in energy than the latter.[19] Ho *et al.* have since published measurements using forward capacitance methods giving evidence for the presence of defect-related interface states.[20] This conclusion has since been challenged by Chantre *et al.*[21] and Werner *et al.*[22]

Hauenstein *et al.*[23,24] and Ospelt *et al.*[25] essentially have confirmed Tung's experimental results: Low barriers (0.62–0.64 eV) were observed for *A*-type and higher barriers (0.69–0.76 eV) for *B*-type oriented interfaces. These papers, however, did not yield new information as to the question whether an observed difference in barrier height was "intrinsic" or just related to the defect concentration at the interface.

Kikuchi *et al.*[26] have provided evidence that a difference could be due to defects. This they concluded from their observation that the barrier height of type-*B* oriented silicide decreases from 0.75 to 0.65 eV as the silicide thickness increases from 50 to 500 Å. For larger thicknesses interface states related to misfit dislocations would cause a lowering of the type-*B* Schottky-barrier height to a defect-dominated value of 0.65 eV; therefore, the barrier height of 0.65 eV at the type-*A* oriented interface is, according to these authors, also dominated by a high defect concentration. Kikuchi *et al.*[27,28] interpret their data in terms of an interface-defect model, using the model as described by Zur *et al.*[29] They conclude that a lowering of the Schottky-barrier height to 0.65 eV requires a density of at least $\sim 3\times10^{13}$ electrically active defects per cm^2 at the interface.

The correlation that Liehr *et al.* made between a high value for the Schottky-barrier height ($\sim$0.80 eV) for *A*-type oriented silicide and the structural perfection of the interface has *not* been confirmed by other groups; moreover, it appears that the results on Schottky-barrier heights by Liehr *et al.* have been influenced by changes in the substrate doping profile caused by the high-temperature surface cleaning treatment employed in that work.[17,18] At present, there is little doubt that the Schottky-barrier heights for both interfaces are different. The fundamental issue whether the difference in barrier height is intrinsically related to the different interfacial atomic arrangements, or just related to a difference in defect density, remains to be solved. Until now, the only defect-sensitive structural probes employed for monitoring the silicide and silicide-silicon interface quality have been cross section and planar-view high-resolution transmission electron microscopy (HRTEM) techniques, which probe a small silicide area. To date, no systematic quantitative studies of the interfacial defect density over large silicide areas have been reported.

In this work we address the issue concerning the origin of the difference in barrier height. We have performed electrical measurements on differently prepared samples using *I-V*, *C-V*, and photoresponse techniques, and have correlated them with the silicide orientation as found by medium-energy ion scattering (MEIS) measurements; in addition, we have probed the quality of both interfaces over a macroscopic area ($\sim$50 mm^2) using MEIS in conjunction with channeling and blocking and observed them to be of very high quality. We present the first experimental evidence that the defect density at the type-*A* interface is smaller than the critical density for defect-dominated pinning of the Fermi level in the band gap; the difference in Schottky-barrier height cannot be explained from the difference in defect density at the type-*A* and type-*B* oriented interfaces. It should therefore be intrinsically related to the atomic symmetry at the interface.

II. EXPERIMENT

First, we describe the experimental setup and procedures used, then the sample preparation.

A. Setup and experimental procedures

The samples were prepared in a multichamber ultrahigh-vacuum system, consisting of a surface analysis chamber, a molecular-beam epitaxy (MBE) apparatus, and a sample loading chamber.[30] The base pressure of this system was 7×10^{-9} Pa. Ni was evaporated using an electron-beam evaporator; in an earlier stage of the experiment sublimation wires were used. During deposition and transfer to the analysis chamber, the pressure did not exceed 3×10^{-7} Pa and quickly recovered afterwards. Sample temperatures were monitored using an infrared pyrometer with an accuracy of 50 °C.

MEIS was employed *in situ* for monitoring the silicide growth process, determination of the silicide orientation obtained, and measurements of the interfacial defect density. The measurements were performed using a 99.8-keV proton or 175-keV He^+ beam collimated to within 0.1°. The sample orientation is controlled by a high-precision UHV three-axis goniometer, enabling alignment of the ion beam with respect to the silicide axes to within 0.1°. The backscattered ions are energy analyzed with a toroidal electrostatic analyzer,[31] enabling simultaneous detection over a 20° range of scattering angles with an angular resolution of better than 0.2° and an angular accuracy of 0.05°. The energy resolution $\Delta E/E$ is 3.6×10^{-3}. The detector can be rotated around the sample by means of a rotary table. By combining scans taken for different angular positions of the analyzer, angular ranges larger than 20° are covered.

The silicide orientation is determined using an ion blocking method initially proposed by van Loenen *et al.*[32] We have labeled the scattering geometries corre-

sponding to both silicide orientations *with respect to ion beam and detector* I and II; the silicides will be referred to as "type I" and "type II" ("type *A*" and "type *B*" refer to interface orientations). Both geometries can be chosen for a given interface orientation by rotating the sample over 180° around the surface normal. The ion beam (175 keV He^+) is incident on the silicide in the $(1\bar{1}0)$ scattering plane with an incident angle α of 24.5° with respect to the surface plane (Fig. 1). This angle does not correspond to a major channeling axis for either of the scattering geometries, so that about equal sensitivities are obtained for both silicide orientations. On their way to the vacuum, the backscattered ions are blocked in directions which are specific for the silicide orientation. For example, silicide in orientation I gives rise to a characteristic blocking minimum at an exit angle β of 35.03°, and the blocking pattern for silicide in orientation II contains a deep minimum at $\beta = 19.3°$ (Fig. 1). In the case of a silicide containing grains of both orientations, the angular distribution of the backscattered ion yield ("blocking pattern") can be described as a weighted average of the characteristic patterns corresponding to type-I and type-II oriented silicides. In an orientation determination experiment, the relative areal fraction of type-I oriented grains $f_I = S_I/(S_I + S_{II})$, in which S_I and S_{II} are the areas of the probed part of the sample occupied by silicides of orientations I and II, respectively, is obtained by comparing the blocking pattern due to backscattering from Ni atoms in a fitting procedure to a weighted average of the calculated Ni-blocking patterns for either of both orientations on an absolute scale. The calculated patterns are obtained using Monte Carlo methods.[33] The error in the areal fraction resulting from such a fit is estimated to be ~8%, which is also the detection limit for grains of opposite orientation in a single-oriented film. Figure 2 shows measured blocking patterns (circles) and fits (drawn lines), both for a type-II oriented film and a film containing grains of type-I and II oriented silicide in about equal amounts. For both *A*- and *B*-type oriented silicide-substrate interfaces, we have obtained areal fractions of the opposite orientation $f_I \leq 0.08$, measured with the silicide in scattering geometry II; after rotation of the sample over 180° around the surface normal (the exchange of geometries I and II), the same analysis yielded an areal fraction of $f_{II} \sim 0.15$. We believe that the former number is reliable, as is concluded from the photoresponse analyses of such samples (see below). A difference in detection limit for detection of type-I oriented grains in type-II material (8%) as compared to the detection limit for type-II grains in type-I oriented silicide (15%) is already expected from the difference in channeling/blocking geometries I and II (Fig. 1), which are differently sensitive to, e.g., small uncertainties in surface relaxations and vibration amplitudes. Consequently, we have analyzed the orientation of our samples of both interfacial orientations with the silicide oriented according to geometry II.

For definition of the diodes we used either evaporation

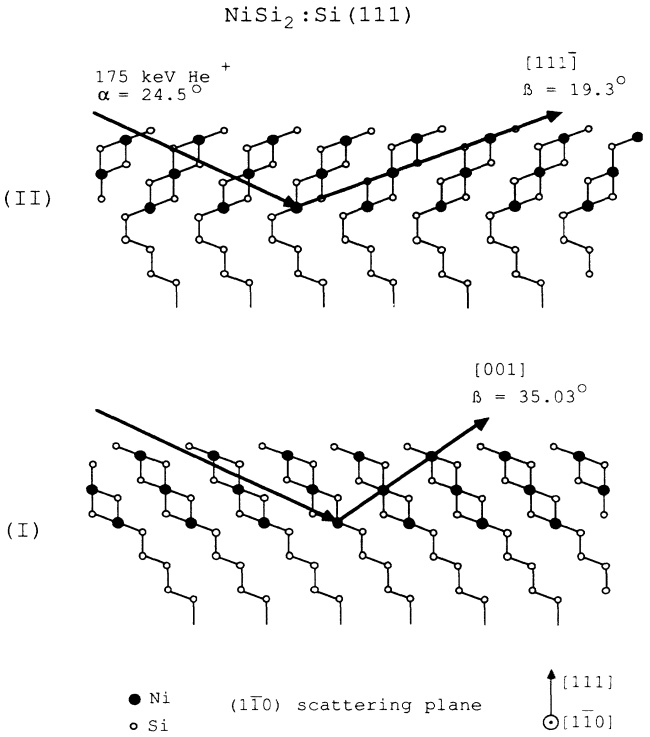

FIG. 1. Scattering geometry used for the orientation determinations in this experiment. Only one $(1\bar{1}0)$ scattering plane is given for either of the two silicide orientations, which are labeled I and II. The ion beam (175 keV He^+) is incident in a direction which is "random" for both silicide orientations. The number of Ni atoms visible to both ion beam and detector shows minima in main crystallographic directions which are specific for the silicide orientation (indicated).

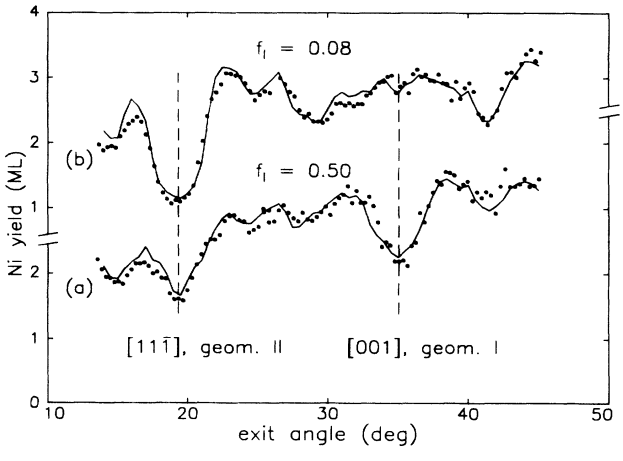

FIG. 2. Two examples of observed blocking patterns (circles) due to backscattering from Ni atoms obtained in the scattering geometry indicated in Fig. 1. Characteristic blocking directions for each of the silicide orientations are indicated. Drawn lines are linear combinations of calculated patterns, assuming a relative areal fraction f_I of regions oriented according to geometry I as indicated. (a) shows the pattern for a silicide which contains 50% of type-I oriented grains; in (b) the pattern from a type-II oriented silicide is given.

masks (stainless steel or Ta) or SiO_2 layers patterned by standard photolithographical methods (Fig. 3). In both cases, a large area (5–20 mm^2) on the sample was available for structure analysis of the silicide. Different diode sizes were prepared with silicide areas ranging from 0.01 to 2 mm^2. Most electrical analyses were performed on diodes of ~ 0.05 mm^2. Back contacts to the substrate were prepared in advance of the experiment by ion implantation (30 keV P^+, 1×10^{15} cm^{-2}). This implantation was electrically activated during the heating stage for surface cleaning (see below). It was used in combination with a thin Ga-In eutectic layer to establish the back contact during electrical analysis; the behavior of the contact was verified to be ohmic.

The electrical analyses were performed in air in a light-shielded case, in which current-voltage (I-V), capacitance-voltage (C-V), and photoresponse (PR) characteristics on the same diode can be measured subsequently without opening the box. The contact to the silicide on the front side is established by positioning a thin Au wire (0.1 mm) on the diode using an optical microscope; the sample table can be moved in the X and Y directions for accurate alignment of the sample with contact wire and light beam. The sample temperature is monitored using a calibrated Pt-100 resistance thermometer.

I-V characteristics were automatically recorded using a Keithley model 230 voltage source and model 619 multimeter in a bias range from -0.5 to 0.5 V; from the characteristics values were deduced for barrier height ϕ_b, ideality factor n, series resistance, and shunt resistance in a computer fit. The latter parameter is useful for analysis of diodes showing some leakage current.

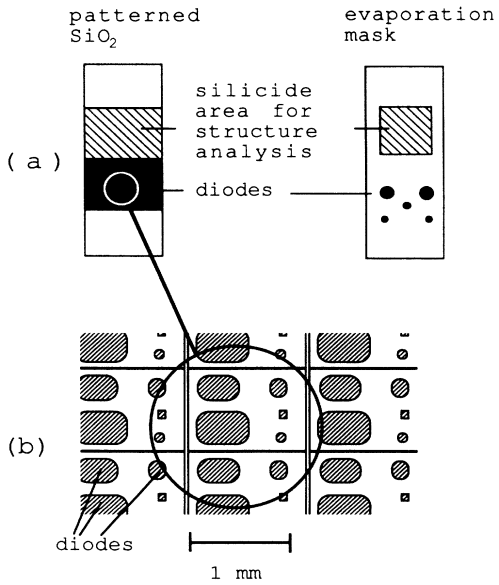

FIG. 3. The sample structures with diode delineation used for the electrical analyses. The sample dimensions are in both cases 7×16 mm^2. (a) SiO_2 pattern (left) and Ta evaporation mask (right); (b) enlarged view of the diode area of the SiO_2 pattern.

For photoresponse analysis a light source was available, delivering monochromatic light with photon energies ranging from 0.62 to 0.97 eV. It consists of a W ribbon lamp, the filament of which is imaged by a lens onto the entrance slit of a computer-controlled grating monochromator (grating 300 lines/mm) and a long-wavelength pass filter ($h\nu < 0.98$ eV). A second lens and a small mirror are used to image the monochromator exit slit onto the diode area. The light beam is chopped at a frequency of 80 Hz. The photon-induced signal from the Schottky diode is measured using a lock-in amplifier (PAR model 121), digitized, and fed into the computer. For normalization of the measured photon-induced signals the system response is monitored using a pyroelectric detector (Molectron 404CM).

Capacitance data at reverse bias were taken using a Hewlett-Packard model 4192A LF impedance analyzer in a frequency range from 0.1 to 2 MHz. The sample was connected to the analyzer in a four-point configuration, to reduce the influence of cable losses.

B. Sample preparation

The samples (n-type, P or As doped, substrate doping levels ranging from 2×10^{14} to 2×10^{16} cm^{-3}) were subjected to a cleaning procedure, involving a degreasing step using high-purity ethanol in an ultrasonic bath and a chemical treatment. The latter has been described by Ishizaka *et al.*[34] and is based on repeated alternating steps of Si oxidation and removal of the thin oxide film formed. The solutions used are HNO_3 at 90 °C and 1% HF at 25 °C, respectively. In this process, also a negligibly small part of the SiO_2 mask is removed. Finally, a volatile oxide is grown, using a solution of H_2O, H_2O_2, and HCl at 90 °C. After each chemical step, the samples are flushed using high-purity water (12–18 MΩ cm) obtained from a Millipore Milli-Q water cleaning system. Baker VLSI-grade chemicals with very low residual particle densities are used throughout. After loading into the UHV system, the thin oxide is evaporated off at a temperature of 800 °C during 10–20 min by direct-current resistive heating. The ion-implanted layer for the back contact is likewise activated during this annealing step. After cleaning, no impurities were detectable using Auger electron spectroscopy [intensity ratios $I(\mathrm{C}(KLL))/I(\mathrm{Si}(LVV))$ and $I(\mathrm{O}(KLL))/I(\mathrm{Si}(LVV))$ smaller than 1×10^{-3}] or MEIS (detection limit $\sim10^{-2}$–10^{-3} monolayer for elements heavier than Si).

Following the recipes given by Tung,[35] A- and B-type oriented silicide layers were grown by deposition of an appropriate amount of Ni at room temperature and annealing to 450–500 °C. In the case of samples without a patterned SiO_2 layer for delineation of the diodes, the mask was used during evaporation.

B-type oriented silicides were obtained by deposition of Ni to an amount of ~4 or $\sim9\times10^{15}$ cm^{-2} (5 or 10 Å); A-type oriented silicides resulted upon annealing of an initially deposited amount of $\sim16\times10^{15}$ cm^{-2} (18 Å). The silicide orientation was checked as described in Sec. II A. Using the electron-beam evaporator at high evaporation speeds (~2 Å s^{-1}) silicides were obtained which

were of single orientation to within 8%, which is the MEIS areal fraction detection limit for detection of silicide grains of opposite orientation (see Sec. II A). Samples with initial coverages differing substantially from the values given above and samples prepared using evaporation wires with much lower Ni yields ($\sim 3\times 10^{-3}$ Å s^{-1}) generally contained mixed silicide layers of which more than $\sim 15\%$ of the total area was occupied by grains of the opposite orientation. This is in agreement with the literature.[35] In the case of the thin *B*-type oriented layers, the silicide thickness was increased to ~ 70 Å using the "template" method,[10,35] to allow for electrical analysis of the samples.

In the case of samples with a patterned SiO_2 layer, the unreacted Ni present on top of the SiO_2 mask after silicide formation was chemically removed to ensure mutual electrical isolation of the diodes. Electrical analysis usually was performed within 24 h after the samples had been exposed to air.

III. RESULTS

Both measurements of electrical characteristics and silicide-substrate interface quality were performed. First we discuss the results of the electrical analyses, then the MEIS measurements of interface quality.

A. Electrical measurements

The electrical characteristics of Schottky-barrier diodes tend to be extremely sensitive to small variations in the preparation conditions. In this experiment, we investigated the electrical properties of some 21 differently prepared samples containing silicide layers of which nine were of *A*-type orientation and seven of *B*-type orientation. Five samples contained grains of both silicide orientations. Most samples were prepared using a SiO_2 mask and contained 96 diodes each. Perfect electrical characteristics were generally, but not always, observed, less perfect diodes being characterized by *I-V* ideality factors $n > 1.20$ and/or leakage current in the reverse characteristic. Diodes with poor *I-V* characteristics were not further considered in the analyses.

All values for barrier heights given are flat-band barrier heights, i.e., the image force has been corrected for; the noncorrected ("observed") barrier height will be referred to as "apparent barrier height."

The *I-V* data reveal convincing dependence of the Schottky-barrier height on interface orientation (Fig. 4). Analysis of the *I-V* behavior of the *A*-type and mainly ($f_A > 0.8$) *A*-type oriented samples results in a Schottky-barrier height of 0.64 ± 0.01 eV with ideality factors $n = 1.02-1.15$. Type-*B* oriented silicide gives rise to a barrier height which shows a larger variation, also over different diodes on one sample, yield an *I-V* barrier height of $\sim 0.72\pm 0.03$ eV, $n \leq 1.10$. Quite linear log(*I*)-*V* behaviors with very low leakage currents are observed for either of both orientations. Layers containing grains of both silicide orientations yield barrier heights which, depending on f_A, vary between 0.65 and 0.68 eV.

Measurements of the photon-induced electron yield also show a dependence of the Schottky-barrier height on interface orientation (Fig. 5). All Fowler curves corresponding to *A*-type oriented silicide show a linear behavior, resulting in Schottky-barrier heights of $\sim 0.64\pm 0.02$ eV. Analysis of *B*-type oriented silicide results in a nonlinear Fowler curve, which does not correspond to a uniform barrier height. This is also observed by Hauenstein *et al.*[23] and Ospelt *et al.*[25] The data can be satisfactorily described as a linear combination of the contributions to the electron yield from regions with "low" and "high" barrier heights ϕ_{bl} and ϕ_{bh}, occupying relative areal fractions of f_{low} and $(1-f_{\text{low}})$ according to

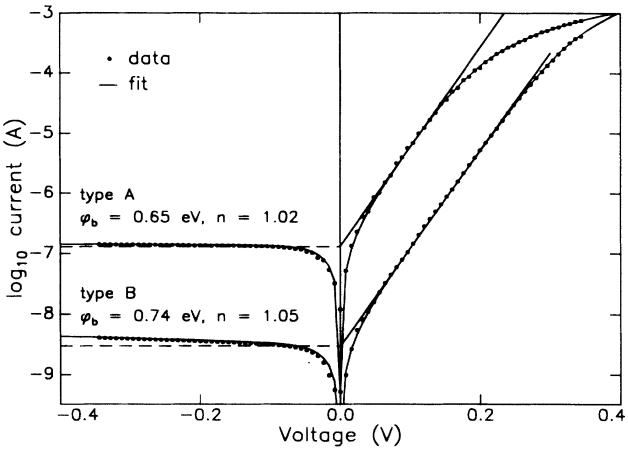

FIG. 4. An example of measured (circles) and calculated (drawn lines) *I-V* data for each of the silicide orientations. The diode area is 3.6×10^{-2} mm^2.

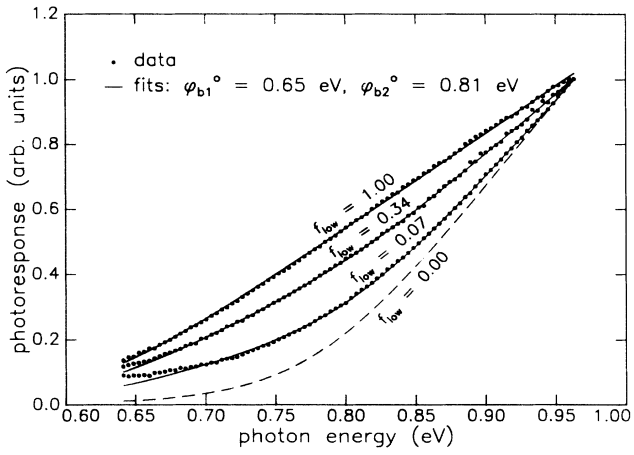

FIG. 5. Photoresponse data (circles) and calculated curves (drawn lines) showing the sensitivity of such data to barrier height nonuniformity. The calculated curves were obtained assuming a two-barrier model using barrier heights of 0.65 and 0.81 eV, respectively, and a relative areal fraction f_{low} of regions with low barrier height. The curves with $f_{\text{low}}=0.00$ and 1.00 show a linear behavior for sufficiently large photon energies. Type-*A* oriented samples yield $f_{\text{low}}=1.00$; analysis of samples with type-*B* orientation results in numbers as small as $f_{\text{low}}=0.07$. A strong correlation between f_{low} and silicide orientation is observed.

$$\Phi = f_{\text{low}}\Phi[(h\nu - e\phi_{bl})/kT] + (1-f_{\text{low}})\Phi[(h\nu - e\phi_{bh})/kT] \ . \quad (1)$$

In this equation, Φ denotes the Fowler function defined by

$$\Phi(\mu) = c \begin{cases} \left[\frac{\pi^2}{6} + \frac{\mu^2}{2} - \left[e^{-\mu} - \frac{e^{-2\mu}}{4} + \frac{e^{-3\mu}}{9} - \cdots\right]\right] & \text{for } \mu \geq 0 \ , \quad (2a) \\ \left[e^{\mu} - \frac{e^{2\mu}}{4} + \frac{e^{3\mu}}{9} - \cdots\right] & \text{for } \mu < 0 \ . \end{cases} \quad (2b)$$

In this equation c is a constant. A computer fit to the photoelectric data indicates at least $\sim 7\%$ of the silicide area of a type-B oriented sample to be occupied by grains with a lower barrier height (0.60–0.65 eV), the rest of the sample area having a barrier height of ~ 0.81 eV. This results in a photoresponse curve with a "bowing" feature (Fig. 5). The areal fraction of the grains with low barrier height can be as high as ~ 0.3, even for well-oriented samples with $f_A = 0.08$. From the parameters of the fit (the apparent barrier heights ϕ_{bl} and ϕ_{bh} and the areal fraction f_{low}) the Schottky-barrier height to be expected from an I-V analysis of the diode can be calculated. Assuming that the observed current can be described as the sum of the contributions from the two regions with different barrier heights, one arrives at[36]

$$\phi_{b,\text{app}} = -\frac{kT}{e} \ln[f_{\text{low}} e^{-e\phi_{bl}/kT} + (1-f_{\text{low}}) e^{-e\phi_{bh}/kT}] \ . \quad (3)$$

In this equation $\phi_{b,\text{app}}$ is the expected apparent barrier height. The observed values for the I-V barrier height of a certain diode are in agreement to within 0.02 eV with the predicted value from photoresponse using this simple model,[37] for all values of f_{low} observed.

An analysis of samples containing silicide grains of both orientations results in photoresponse curves which can be described well in terms of the same model assuming two different flat-band barrier heights with values $\phi_{bl} = 0.65$ eV and $\phi_{bh} = 0.81$ eV. Observed I-V values for the Schottky-barrier height are again in good agreement with the prediction derived from photoelectric data. The areal fraction occupied by domains of low barrier height is consistent to within 20% with the areal fraction of A-type oriented silicide as determined using MEIS. In those cases in which a deviation of f_{low} from f_A was observed, f_{low} was larger than f_A, indicating that the barrier height is locally pinned to a lower value (see below).

The results from C-V analysis of our samples are less clear cut. Although in most cases the slope of the plot of C^{-2} against V agrees with the substrate doping levels used, the Schottky-barrier heights obtained using this technique were generally 0.05–0.1 eV higher than the C-V values predicted from photoresponse analysis of the diodes. In some cases nonlinear plots of C^{-2} against V are obtained, making a determination of the barrier height impossible. Annealing temperatures for surface cleaning used in this experiment were $\sim 800\,^{\circ}\text{C}$, so that the problem is *not* related to dopant segregation.

In summary, from our photoresponse and current-voltage data we conclude that the flat-band barrier heights of type-A and type-B oriented interfaces are 0.65 and ~ 0.81 eV, respectively. The relative areal fraction f_{low} of regions with the low barrier height as determined using photoresponse is generally consistent with the relative areal fraction of type-A oriented regions in the silicide as determined using ion scattering. The fits to photoresponse curves indicate that the barrier height corresponding to the purely type-B oriented interface amounts to 0.81 eV. The data indicate that a nonnegligible fraction (at least $\sim 7\%$) of the sample area is occupied by regions having a barrier height of ~ 0.64 eV. We could ascribe this contribution to $\sim 7\%$ of the area of a type-B oriented sample to be of type-A orientation. However, a part of type-B oriented silicide having low barrier height could also be related to defects present as the type-B oriented interface, e.g., due to steps at this interface, locally lowering the barrier height. This is consistent with a slightly higher defect concentration at this interface (see Sec. III B). Observed I-V barrier heights are in good agreement with those expected from the two-barrier model. Our conclusions are in quantitative agreement with the results by Hauenstein *et al.*[24] and Ospelt *et al.*[25]

B. Search for interface defects

In order to investigate the degree of crystalline perfection of the $NiSi_2$/Si(111) interfaces, we performed a MEIS experiment on samples without diodes, so that a large silicide area (~ 50 mm^2) was available for structural analysis.

The experiment was performed in the $(1\bar{1}0)$ scattering plane using protons with a primary energy of 99.8 keV. The ion beam was aligned with the $[\bar{1}\,\bar{1}\,\bar{1}]$ (normal) crystal axis, in order to reduce the hitting probability of the atoms on lattice sites and to obtain a high sensitivity to displaced atoms. The detector was set around the $[11\bar{1}]$ axis in the silicide to further enhance the sensitivity. This particular set of channeling/blocking axes (see Fig. 6) was chosen for the following reason.

Due to an in-plane elastic stretching of the $NiSi_2$ lattice to match the Si substrate lattice, the off-normal crystal axes in the silicide are slightly tilted toward the surface plane. Consequently, for type-A oriented silicide these axes do not exactly coincide with their counterparts in the Si substrate lattice, but have a slightly different direction. This causes an enhanced dechanneling of ions traveling along such axes once they enter the substrate from the silicide. The only crystal axis which has exactly the same direction in silicide and silicon is the $[\bar{1}\,\bar{1}\,\bar{1}]$ axis. Therefore this entrance axis offers a very small dechanneling probability for ions entering the substrate. Of course, the stretching of the lattice does affect the detection probability of protons backscattered from substrate lattice-site atoms along the $[11\bar{1}]$ outgoing direction. The angular shift of this axis amounts to 0.15°. Both the $[\bar{1}\,\bar{1}\,\bar{1}]$ and the $[11\bar{1}]$ directions are very efficient $\langle 111 \rangle$-

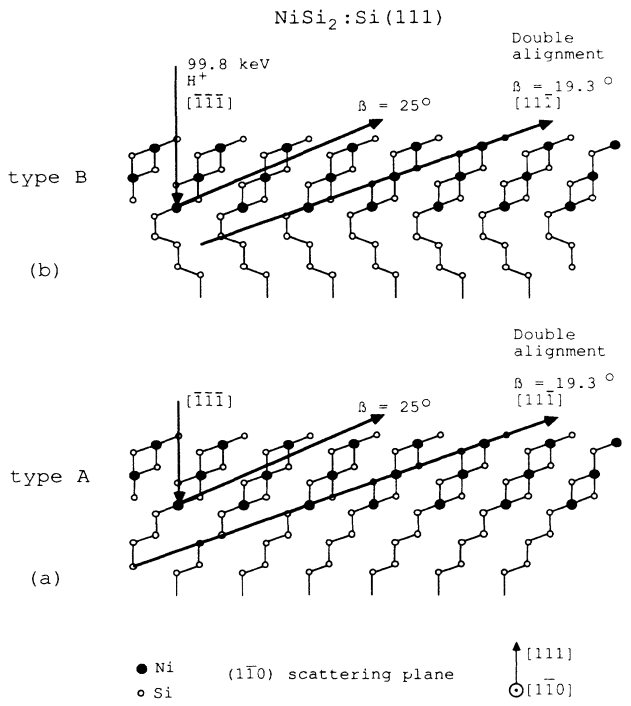

FIG. 6. Scattering geometry used in the determinations of the interface quality. The proton beam (99.8 keV primary energy) is incident in the direction along the surface normal. Indicated are the exit directions used in this experiment. Note that the [11$\bar{1}$] outgoing direction in type-*B* oriented silicide is not a main crystallographic direction in the Si substrate.

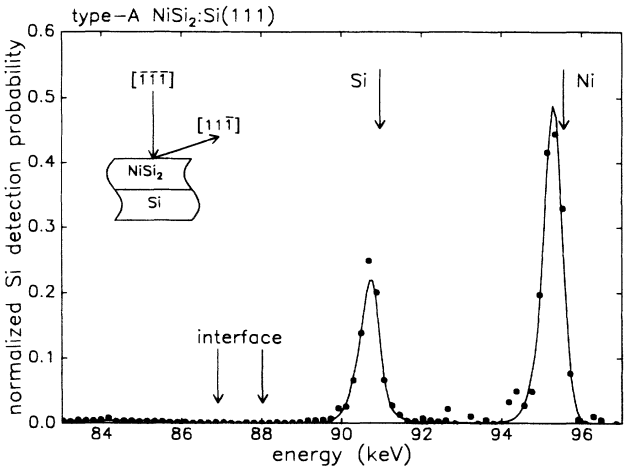

FIG. 7. Energy spectrum taken on type-*A* oriented silicide along the [11$\bar{1}$] outgoing direction (Fig. 6), showing measured data (circles) and a calculated curve (drawn line). The latter has been obtained using Monte Carlo techniques (see text). Indicated is the position of the interface in the Si signal, which is studied in more detail in Figs. 8 and 9.

type blocking axes, resulting in a very low yield from atoms on lattice sites, and, due to a high ion flux in the crystal channels, in an enhanced yield from atoms which are significantly displaced from lattice sites.

For type-*B* oriented silicide the situation is slightly different. The [$\bar{1}\bar{1}\bar{1}$] direction in the silicide again remains unchanged, so that the substrate atoms are shadowed equally well. The direction of the type-*B* [11$\bar{1}$] silicide blocking axis, however, does not correspond to that of a major blocking axis in the substrate, as is the case for the type-*A* oriented interface [see Fig. 6(b)]. Consequently, along this axis the detection probabilities of ions backscattered from silicide atoms are identical to those in the type-*A* case, but the backscattering yield from *substrate* atoms increases with increasing depth as compared to the type-*A* oriented interface, because the backscattered ions are not blocked on their way through the substrate.

Figure 7 shows an energy spectrum of the backscattered ion yield taken from a type-*A* oriented sample with a silicide thickness of 63 Å. The channeling/blocking geometry is that of Fig. 6(a). Because of the different masses of Ni and Si atoms, the corresponding surface peaks show up at different energies. Ion backscattered from atoms residing deeper in the bulk lose energy due to electronic interactions ("stopping") as they travel through the crystal and show up at lower energies in the energy spectrum. As was pointed out in the previous paragraph, the detection probability of such atoms is very small ($\sim 5\times 10^{-4}$) for a perfect crystal. The backscattered ion yield behind the surface peak ("minimum yield") is therefore directly indicative of crystal quality, and from this spectrum it is already clear that the quality of the silicide is excellent. The drawn line is a spectrum obtained from Monte Carlo computer simulations and will be discussed below. The arrows indicate the expected position of the silicide/silicon interface in the Si signal, as calculated for ordered interface atoms ($\sim$87 keV) and disordered atoms at the interface ($\sim$88 keV). No interfacial disorder is evident from this spectrum.

In order to investigate the quality of the interfaces in more detail, we have performed an experiment on the interface region using the Si signal (Figs. 8 and 9). For each of the silicides both the cases of double alignment ([11$\bar{1}$]-direction, exit angle $\beta = 19.3°$), and single alignment ($\beta = 25.0°$) are considered. The parts of the spectra not shown are virtually identical for both orientations (equal silicide thicknesses of $\sim$63 Å were analyzed in this experiment). The data taken at 19.3° [Figs. 8(a) and 8(c)] demonstrate that indeed the parts of the spectra showing the minimum yields due to the silicide (energy range 87–89 keV) are identical, and that in the case of the type-*B* crystal the minimum yield is higher below this energy range. Little or no difference is observed between the spectra for both orientations in the "random" outgoing direction corresponding to 25.0° exit angle [Fig. 8(b) and 8(d)].

All of these data are accurately reproduced by Monte Carlo computer simulations on perfectly ordered crystal models.[33,38] In such a simulation a representative set of ion trajectories through a crystal slab is constructed. For each of the ion tracks, collision probabilities[33] and elastic and inelastic energy losses of the ions are evaluated. It is well known that the energy losses are dependent on the ion trajectories through the crystal.[32] For instance, for an ion which is backscattered from a lattice site to be

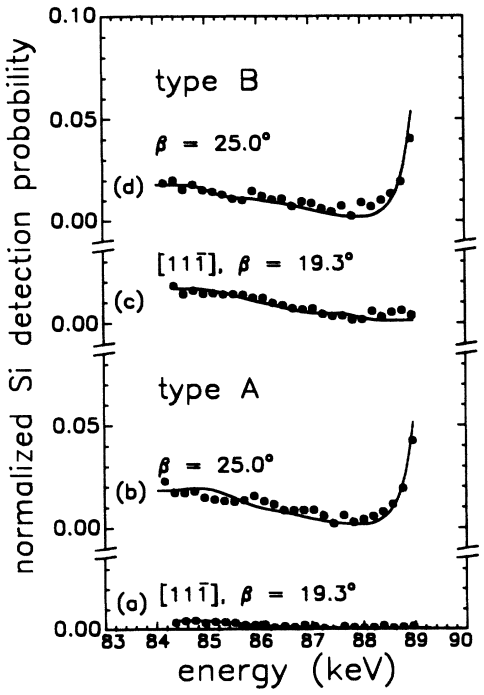

FIG. 8. Si signal for both orientations, showing the detection probability of the Si atoms at different depths in double ([11$\bar{1}$], exit angle $\beta=19.3°$) and single ($\beta=25.0°$) alignment. Data points are indicated by circles. The calculated curves are described in the text.

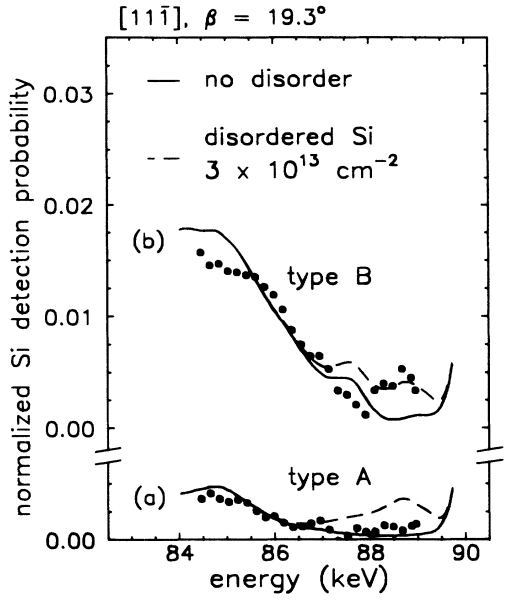

FIG. 9. The spectra of Figs. 8(a) and 8(c) in an enlarged view, showing the defect detection sensitivity in double alignment ([11$\bar{1}$] silicide outgoing direction) for both interface orientations. Calculated curves are given for a perfectly ordered crystal (drawn curves) and for a model in which a concentration of 3×10^{13} Si atoms cm^{-2} is visible to ion beam and detector at the interface (dashed curves).

detected in a major crystal direction, it must have traveled along a trajectory close to the atomic strings where the electronic density is relatively high. Therefore such an ion will have lost a relatively large amount of energy. If, on the other hand, the ion is backscattered from atoms which reside in the center of the crystal channels (e.g., defected atoms), where the electronic density is much smaller, it will lose a relatively small amount of energy. The computer code used here assumes an ion-atom impact-parameter-dependent inelastic energy loss which obeys the semiempirical exponential relationship given by Oen and Robinson.[39] The energy-loss function is normalized such that it reproduces the random stopping power.[40] The spectra are constructed taking into account the contributions from different isotopes of the elements. Additional "smearing" effects like multiple collisions and Doppler broadening have been taken into account; the detector resolution (full width at half maximum 360 eV) is modeled as a Gaussian. The energy loss at a fixed ion-atom impact parameter is assumed to be statistically spread around its mean value (the calculated spectra are influenced only weakly by this spread; the energy straggling introduced by the impact-parameter dependence of the energy losses and the detector resolution dominate the energy spread in this particular case). The energy spectra obtained from the simulations are in good agreement with experimental data, both as regards absolute intensities[33] and energy losses involved.[38]

In the simulation of this experiment, one-dimensional root-mean-square (rms) vibration amplitudes of 0.095 and 0.110 Å have been assumed for the Ni and Si atoms in the silicide, respectively; for the vibration amplitudes of the Si substrate atoms a value of 0.078 Å has been taken. These values are identical to those used in previous studies.[32] Both the calculated spectra and experimental data, after background subtraction, were normalized to the Si random height, using tabulated values for the stopping of protons in Si.[40] The results are given in Figs. 7–9. Striking quantitative agreement between simulations and experimental data is obtained throughout for the ordered model, for both single and double alignment and for both silicide orientations (Fig. 8); for the case of type-*B* silicide in double alignment ([11$\bar{1}$] axis), the higher yield from the substrate atoms ($E<87$ keV) is also accurately described.

The low minimum yield in double alignment results in a high efficiency for the detection of defects. Figure 9 shows the data for both interface orientations in an enlarged view. The simulations for perfectly ordered interfaces (drawn curves) are in good agreement with the data. Upper limits for the interfacial defect concentrations will be derived in the following paragraph.

In this experiment the "relative detection efficiency," i.e., the number of detected atoms per displaced atom, is larger than 1 due to several reasons. We will discuss some conceivable types of defects and estimate their relative detection efficiency. *Interstitial atoms* are detected with an enhanced detection probability, due to ion focusing effects both on the incoming and outgoing tracks (the full incident and backscattered ion flux is confined to the crystal channels, giving high collision probabilities there; this is experimentally demonstrated in Ref. 12). Using

the computer simulations of the experiment, we have calculated the ion fluxes in the centers of the crystal channels to amount to up to 3 times the incident ion flux both on the incoming and outgoing directions. If we neglect associated strain fields, we arrive at a relative detection efficiency of at least 2–3. *Point defects other than interstitials* are detected with a similar efficiency as regards direct scattering and additionally may give rise to strain fields in the crystal such that crystal channels are bent, resulting in an enhanced dechanneling probability and therefore an increased yield. *Misfit dislocations and stacking faults at the interface* are detected with very high sensitivity. Apart from the many displaced atoms involved, in this case complete substrate atom strings are visible to the high-flux ion beam, giving rise to ion yields equivalent to 3–4 atoms per displaced atom. From these considerations, an equivalent ion yield of at least 2–3 detected atoms per displaced atom is to be expected. Therefore, we have conservatively assumed a relative detection efficiency of 2 in this analysis.

In Fig. 9 the spectra which are to be expected from samples containing a concentration of 3×10^{13} cm^{-2} of disordered Si atoms located at the interface are given (broken lines). From the data we conclude that the number of displaced atoms at the type-*A* oriented $NiSi_2$/Si(111) interface [see Fig. 9(a)] must be smaller than the equivalent of 1% of a monolayer, which is $\sim1\times10^{13}$ cm^{-2}. The density of specific types of defects, e.g., misfit dislocations, is even smaller. The defect density given is a *total* concentration in a few layers at the interface. The spectrum from the type-*B* oriented interface in double alignment [Fig. 9(b)] shows a slightly enhanced yield in the energy range around 88.5 keV, indicative of the presence of a small concentration of disordered atoms at the interface or in the silicide. From the data the concentration of displaced atoms at the interface is estimated to be at most 3×10^{13} cm^{-2}. Because steps are always present at a real (slightly misoriented) surface, a higher defect concentration at the type-*B* oriented interface is expected because steps with a height of one or two (111) layers necessarily give rise to dislocations at the interface.

It is reasonable to assume that the number of electrically active interface states associated with the defected atoms is at most one per defected atom; that means that the interface state concentration is equal to or smaller than the numbers given above: less than $\sim1\times10^{13}$ cm^{-2} for type-*A*, and less than $\sim3\times10^{13}$ cm^{-2} for type-*B* oriented silicide.

The upper limits for the defect concentrations obtained from our experiment should be compared to the defect concentrations required to pin the Fermi level in the band gap (for metal-Si contacts, defect states are believed to pin the Fermi level at an energy level of 0.62 eV below the conduction-band edge at the interface,[28,41] so that defects *lower* the barrier height on *n*-type Si in this case). Zur *et al.*[29] have calculated the Fermi-level position in the band gap as a function of the interface defect density, both for submonolayer coverage and thick films of metal. For the latter case they conclude that the critical defect density for Fermi-level pinning is $\sim10^{14}$ cm^{-2}. Using exactly the same scheme, Kikuchi[27,28] has calculated that for a lowering of the barrier of a $NiSi_2$/Si(111) interface from 0.79 (type *B*) to 0.65 eV (type *A*), a change in defect density from $\sim3\times10^{12}$ (type *B*) to $\sim3\times10^{13}$ cm^{-2} (type *A*) is required. The fact that high defect densities are required for Fermi-level pinning is related to the associated energy levels for charge transfer being spread over the band gap in a broad distribution. Our experiment shows that the defect density at the type-*A* oriented interface is significantly lower than these critical values; therefore, it is too small to explain a lowering of the barrier height from 0.79 to 0.65 eV. Moreover, a higher instead of a lower barrier height is observed for type-*B* oriented silicide, which has the higher defect density. This is inconsistent with a model in which the *A* and *B* type $NiSi_2$/Si(111) barrier height difference is solely caused by defects.[6,27,28,41]

It has been argued by Kikuchi *et al.* that defects, present in thick (~500 Å) type-*B* oriented silicide layers, are responsible for a significant lowering of the Schottky-barrier height.[26] We also have experimental evidence in support of this for thin type-*B* oriented films (70 Å) in which defects were introduced by ion bombardment. Additionally, we note that the presence of regions with a low barrier height on type-*B* oriented samples (see Sec. III A) can be associated with the local presence of defects, which is consistent with our measurements of defect density.

We conclude that the difference in Schottky-barrier height between both interface orientations cannot be explained from a higher defect density at the type-*A* oriented interface as compared to type *B*. Hence, the difference should have an intrinsic origin; defects at these interfaces, however, do significantly affect Schottky-barrier height.

In summary, the type-*A* and type-*B* oriented silicides are found to be structurally of high quality; there is no evident for atoms displaced from lattice positions to within 1×10^{13} cm^{-2} for the type-*A* oriented interface. The defect density at the type-*B* oriented interface is smaller than 3×10^{13} cm^{-2}. It is concluded that the difference in Schottky-barrier height between type-*A* and type-*B* oriented interfaces is intrinsically related to the interface atomic arrangement.

IV. DISCUSSION

Epitaxial $NiSi_2$/Si(111) is the first evidently nondefect-dominated metal-semiconductor model system. This has important consequences for the description of its electric properties. The absence of defect-related pinning at the interface enables the barrier height to be fully determined by intrinsic mechanisms.

In the years following the discovery of the *A*- and *B*-type $NiSi_2$/Si(111) barrier height difference,[16] several experimental and theoretical papers have contributed to explaining an intrinsic difference.[42–46] Werner[43] has experimentally shown that the barrier height dependence on interface bond length is too small to explain the difference in terms of different silicide-silicon distances for both orientations.

In our view, the long-range order at the interface plane, related to the small density of defects, gives rise to

a strong two-dimensional interface state which has a well-defined energy in the band gap, such that the local density of states shows a distinct peak. The state should be strong enough to influence or "pin" the position of the Fermi level in the band gap. The nature of such a surface state is directly related to the interaction between the three-dimensional electron states in metal and semiconductor, which obey spatial translational and rotational symmetry rules imposed by the crystal. Das *et al.*[45] have performed band-structure calculations for the two different interfaces. An interface band is calculated having a semidangling bond character, related to the sevenfold coordination number of the interface Si atoms. The position of this band relative to the conduction-band edge is different for both interface orientations. These authors calculate a difference in barrier height of 0.14 eV between both interfaces, in agreement with experiment. However, the absolute values of the barrier heights are in error by as much as 0.4 eV. The interface band gives rise to a dipole in the semiconductor near the interface which is different for both orientations. The presence of such an orientation-dependent dipole is also suggested by Yeh.[46]

Recently, a second system which shows a strong dependence of Schottky-barrier height on interface structure has been discovered.[47] In that work, the barrier heights of differently prepared Pb/Si(111) interfaces have been shown to differ by as much as 0.23 eV. The anomalously high value of the Schottky-barrier height at a Si(111)$(\sqrt{3}\times\sqrt{3})R$ 30°-Pb interface (0.93 eV) is attributed to pinning of the Fermi level by an intrinsic electronic state in the band gap at an energy of 0.93 eV below the conduction-band edge. This explanation is perfectly consistent with the picture for the behavior of the $NiSi_2$/Si(111) interface as given above.

V. CONCLUSIONS

In this experiment we have confirmed that the barrier heights of nonrotated and rotated epitaxial $NiSi_2$/(111) films on *n*-type Si(111) are 0.65 and ~0.81 eV, respectively. Measurements of the interfacial defect density show that the silicide-silicon interfaces are of very good quality. As a result of this work, it is concluded that the difference in Schottky-barrier height cannot be explained in terms of interface defect states, but instead is intrinsically related to the different atomic configurations at the interfaces.

ACKNOWLEDGMENTS

P. F. A. Alkemade (University of Western Ontario, London, Western Ontario, Canada) is gratefully acknowledged for the development of the Monte Carlo computer code used for evaluation of the inelastic ion-energy losses. A. E. M. J. Fischer and L. F. Tiemeyer are acknowledged for important contributions to this work. The authors have greatly benefited from discussions with I. Ohdomari (Waseda University, Tokyo, Japan) and J. W. M. Frenken. This work is part of the research program of the Foundation for Fundamental Research on Matter (FOM) and was made possible by financial support from the Dutch Organization for the Advancement of Research (NWO).

[1]W. Schottky, Naturwissenschaften **26**, 843 (1938).
[2]N. F. Mott, Proc. Cambridge Philos. Soc. **34**, 568 (1938).
[3]J. Bardeen, Phys. Rev. **71**, 717 (1947).
[4]V. Heine, Phys. Rev. **138**, A1689 (1965).
[5]J. Tersoff, Phys. Rev. Lett. **52**, 465 (1984).
[6]W. Mönch, Phys. Rev. Lett. **58**, 1260 (1987).
[7]S. G. Louie, and M. L. Cohen, Phys. Rev. B **13**, 2461 (1976).
[8]R. E. Allen and J. D. Dow, Phys. Rev. B **25**, 1423 (1982).
[9]W. E. Spicer, I. Lindau, P. Skeath, C. Y. Su, and P. Chye, Phys. Rev. Lett. **44**, 420 (1980).
[10]R. T. Tung, J. M. Gibson, and J. M. Poate, Phys. Rev. Lett. **50**, 429 (1983).
[11]D. Cherns, G. R. Anstis, J. L. Hutchinson, and J. C. H. Spence, Philos. Mag. **46A**, 849 (1982).
[12]E. J. van Loenen, J. W. M. Frenken, J. F. van der Veen, and S. Valeri, Phys. Rev. Lett. **54**, 827 (1985).
[13]E. Vlieg, A. E. M. J. Fischer, J. F. van der Veen, B. N. Dev, and G. Materlik, Surf. Sci. **178**, 36 (1986).
[14]I. K. Robinson, R. T. Tung, and R. Feidenhans'l, Phys. Rev. B **38**, 3632 (1988).
[15]J. Zegenhagen, K.-G. Huang, W. M. Gibson, B. D. Hunt, and L. J. Schowalter, Phys. Rev. B **39**, 10 254 (1989).
[16]R. T. Tung, Phys. Rev. Lett. **52**, 461 (1984).
[17]R. T. Tung, K. K. Ng, J. M. Gibson, and A. F. J. Levi, Phys. Rev. B **33**, 7077 (1986).
[18]M. Liehr, P. E. Schmidt, F. K. Legoues, and P. S. Ho, Phys. Rev. Lett. **54**, 2139 (1985).
[19]D. R. Hamann, Phys. Rev. Lett. **60**, 313 (1988).
[20]P. S. Ho, E. S. Yang, H. L. Evans, and X. Wu, Phys. Rev. Lett. **56**, 177 (1986).
[21]A. Chantre, A. F. J. Levi, R. T. Tung, W. C. Dautremont-Smith, and M. Azlowar, Phys. Rev. B **34**, 4415 (1986).
[22]J. Werner, A. F. J. Levi, R. T. Tung, M. Anzlowar, and M. Pinto, Phys. Rev. Lett. **60**, 53 (1988).
[23]R. J. Hauenstein, T. E. Schlesinger, T. C. McGill, B. D. Hunt, and L. J. Schowalter, Appl. Phys. Lett. **47**, 853 (1985).
[24]R. J. Hauenstein, T. E. Schlesinger, T. C. McGill, B. D. Hunt, and L. J. Schowalter, J. Vac. Sci. Technol. A **4**, 860 (1986).
[25]M. Ospelt, J. Henz, L. Flepp, and H. von Känel, Appl. Phys. Lett. **52**, 227 (1988).
[26]A. Kikuchi, T. Ohshima, and Y. Shiraki, J. Appl. Phys. **64**, 4614 (1988).
[27]A. Kikuchi, Phys. Rev. B **39**, 13 323 (1989).
[28]A. Kikuchi, Phys. Rev. B **40**, 8024 (1989).
[29]A. Zur, T.C. McGill, and D. L. Smith, Phys. Rev. B **28**, 2060 (1983).
[30]P. M. J. Marée, A. P. de Jongh, J. W. Derks, and J. F. van der Veen, Nucl. Instrum. Methods Phys. Res. Sect. B **28**, 76 (1987).
[31]R. G. Smeenk, R. M. Tromp, H. H. Kersten, A. J. H. Boerboom, and F. W. Saris, Nucl. Instrum. Methods Phys. Res. Sect. **195**, 581 (1982).

[32]E. J. van Loenen, A. E. M. J. Fischer, J. F. van der Veen, and F. Legoues, Surf. Sci. **154**, 52 (1985).
[33]J. W. M. Frenken, R. M. Tromp, and J. F. van der Veen, Nucl. Instrum. Methods Phys. Res. Sect. B **17**, 334 (1986).
[34]A. Ishizaka, and Y. Shiraka, J. Electrochem. Soc. **133**, 666 (1986).
[35]R. T. Tung, J. Vac. Sci. Technol. A **5**, 1840 (1987).
[36]I. Ohdomari and K. N. Tu, J. Appl. Phys. **51**, 3735 (1980).
[37]This approach is valid provided that the average size of single-barrier height domains is not too small in comparison with the Debye screening length; see I. Ohdomari and H. Aochi, Phys. Rev. B **35**, 682 (1987).
[38]P. F. A. Alkemade (unpublished).
[39]O. S. Oen, and M. T. Robinson, Nucl. Instrum. Methods **132**, 647 (1976).
[40]J. F. Ziegler, J. P. Biersack, and U. Littmarck, *The Stopping and Range of Ions in Matter* (Pergamon, New York, 1985).
[41]P. E. Schmidt, Helv. Phys. Acta **58**, 371 (1986).
[42]Xu Yongnian, Zhang Kaiming, and Xie Xide, Phys. Rev. B **33**, 8602 (1986).
[43]J. H. Werner, Appl. Phys. Lett. **54**, 1528 (1989).
[44]N. V. Rees and C. C. Matthai, Semicond. Sci. Tech. **4**, 412 (1989).
[45]G. P. Das, P. Blöchl, O. K. Andersen, N. E. Christensen, and O. Gunnarsson, Phys. Rev. Lett. **63**, 1168 (1989).
[46]J. J. Yeh, Appl. Phys. Lett. **55**, 1241 (1989).
[47]D. R. Heslinga, H. H. Weitering, D. P. van der Werff, T. M. Klapwijk, and T. Hibma, Phys. Rev. Lett. **64**, 1589 (1990).